Direct Imaging of Exoplanets: Science & Techniques
Proceedings IAU Colloquium No. 200, 2005
C. Aime and F. Vakili, eds.

doi:10.1017/S1743921306009550

Current status of the coronagraphic mode for the 3.5m SPICA space telscope

L. Abe[1], M. Tamura[1], T. Nakagawa[2], K. Enya[2], S. Tanaka[2], K. Fujita[3], J. Nishikawa[4], N. Murakami[4], H. Kataza[2] and The SPICA Working Group

[1]Infrared and Optical Astronomy Division & Extrasolar Planet Project Office, National Astronomical Observatory of Japan, Ōsawa 2-21-1, Mitaka-city, 181-8588 Tōkyō, Japan
contact email: abe@optik.mtk.nao.ac.jp

[2]Department of Infrared Astrophysics, Institute of Space and Astronautical Science, Japan Aerospace Exploration Agency Yoshinodai 3-1-1, Sagamihara, Kanagawa, 229-8510, Japan,
contact email: enya@ir.isas.jaxa.jp

[3]Graduate School of Science & Technology, Kobe University, Nada Kobe 657-8501 Japan

[4]MIRA Project, National Astronomical Observatory of Japan, Ōsawa 2-21-1, Mitaka-city, 181-8588 Tōkyō, Japan

Abstract. As of early ∼2010's, the Japanese SPace Infrared telescope for Cosmology and Astrophysics (SPICA) space observatory will be launched. This actively cooled, cryogenic (4.5K), 3.5m telescope will operate in the mid and far infrared spectral regions. With its very high sensitivity, one of SPICA's aims will be the direct detection and characterization of extra-solar outer planets of nearby stars. The goal contrast ranges from 10^5 to 10^6 up to an angular separation of ∼5 arcsec. The relatively low angular resolution at MIR (5 to 20 μm) requires an efficient and robust coronagraphic mode working at cryogenic temperatures. In this presentation we describe several envisaged preliminary designs and assess their performance against the science goals and host telescope specifications. These are compared against numerical simulations and instrumental environment considerations, such as the need for an actively corrected wavefront.

Keywords. Instrumentation: adaptive optics, Instrumentation: high angular resolution, Technique: high angular resolution, Telescopes.

1. Introduction

Japan have put efforts in this direction and established a long term roadmap toward earth-like planet direct observation and characterization with its JTPF (Japanese Terrestrial Planet Finder) project. But the efforts have already started in that direction some years ago with the ground based coronagraphic facility CIAO installed at the focus of the 8.3m Subrau telescope in Hawaii. The roadmap gathers both ground based and space based observatories. In a very near future (from year 2007), the CIAO coronagraph will be replaced by the next generation HiCIAO instrument (see Tamura *et al.*, these proceedings) which will benefit both from a new adaptive optics system (188 actuators, curvature sensor WFS), and from the excellent seeing atop Mauna Kea. Spectral and polarization simultaneous differential imaging is expected to provide contrasts up to 10^6 between below 1.0" in the nIR bands (JHKs). Further ahead, the 3.5m SPICA space telescope will hopefully host a dedicated coronagraph instrument which studies have just started in late 2004. This mIR to sub-millimeter (5μm to 200μm) cryogenic telescope will have an equivalent sensitivity to JWST below 25μm and will benefit from a monolithic pupil.

2. The SPICA telescope

The SPICA telescope will be launched in the early 2010's onboard an HIIA rocket (Nakagawa, 2000, Tamura, 2000). Many efforts were dedicated to the study of the cryogenic system of the telescope to cool it down to 4.5K. These cryogenic temperature implies a number of constraints on the optics and especially for the coronagraphic part which needs a high quality wavefront prior to enter the coronagraph itself. The primary optics (primary and secondary mirrors), as well as supporting structures will be made of either SiC or C/SiC (Carbon/Silicon carbide). Cryogenic tests of deformation at 4.5K are undergoing at ISAS. Moreover, the cryo-cooler will generate some vibrations producing a large pointing error of about 3" which is much too large for the coronagraphic requirements. To solve this problem, a cryogenic tip-tilt mirror will be used which is expected to correct the tip-tilt jitter down to 0.03". Further details can be found in Enya *et al.*, these proceedings.

3. The SPICA mission

SPICA will be used to study many astrophysical domains, ranging from proto-planetary systems to extragalactic sources. Amongst these goals, the coronagraphic instrumentation will be dedicated to the direct detection and characterization of outer extrasolar planets. For stars within 10pc, the exploration field will be set by the spectral band, and by the coronagraph potential in terms of Inner and Outer Working Angles (IWA and OWA, see below for coronagraphic devices). With a 10pc distance, at the lowest wavelength (5μm), the diffraction limit corresponds to a planet distance of 3AU. Considering that the coronagraph IWA is at most $1.5\lambda/D$, the smallest possible IWA will be around 5AU. Under the current specifications for the telescope optics, the OWA will probably limited by the DM specification and/or by the coronagraph type to be used (see below). At the present, the baseline OWA is set to around $10\lambda/D$, which corresponds to 30AU for a 10pc at 5μm and more than 100AU at 20μm (but the IWA will also increase to 12AU in the best cases). Provided a contrast of 10^6 can be reached within this exploration field, the possible targets are self luminous planets of ages between $1 \sim 2$Gy and around a few Jupiter masses.

4. Coronagraph requirements

Due to the limited angular resolution of the telescope from 5 to 20μm, the coronagraph needs to be sensitive at low *inner working angles* (IWA). But the high residual tip-tilt jitter does not allow certain coronagraphic concepts such as AIC (Gay & Rabbia, 1996) or Roddier&Roddier (Roddier & Roddier, 1997) coronagraphs. The tip-tilt jitter will be mainly due to the vibrations caused by the cryo-cooler devices. The estimated pointing stability is only 1 arcmin, whilst the envisaged tip-tilt mirror correction will provide a 60mas residual ($\lambda/10$ @ 10μm). The current telescope design includes a 20% central obscuration associated with a cross-shaped spider support. Under these conditions, only a few solutions can be envisaged. Most very efficient coronagraphs (e.g. AIC, Phase Mask) are too sensitive to tip-tilt jitter (30 mas) to provide a stable high contrast coronagraphic image. The four quadrant phase mask is also too handicapped by the large central obscuration and maybe too sensitive to the residual tip-tilt jitter. Our choice focused on coronagraphs which are poorly or moderately sensitive to tip-tilt errors, and with the lowest possible inner working angle. The most challenging concept which is currently planned for tests is the Multi-Stage Apodized Lyot Coronagraph (Aime &

https://doi.org/10.1017/S1743921306009550 Published online by Cambridge University Press

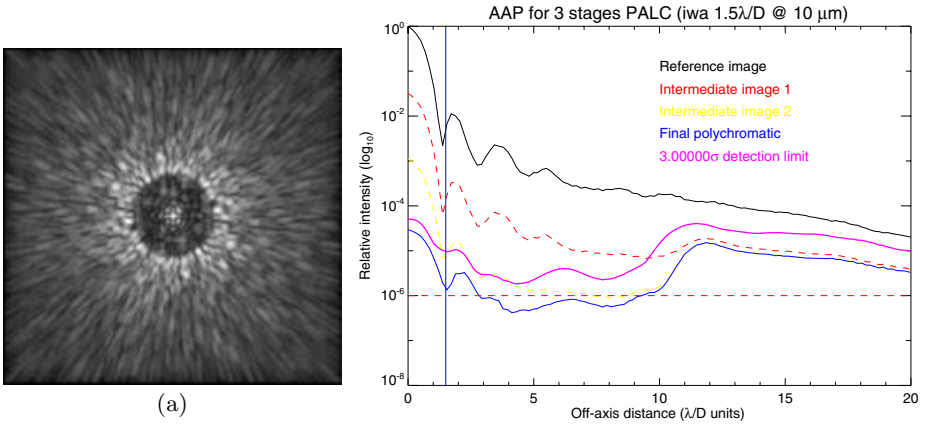

Figure 1. Numerical simulation of the SPICA with a 3S-PALC coronagraph between 9μm and 10μm: (a) final polychromatic image (non linear intensity scale) and (b) azimuth averaged profiles including intermediate stages profiles. The 3-σ limit includes the residual speckle intensity fluctuations.

Soummer, 2004). The optical complexity and marginally the throughput are the main drawbacks of this concept (see next section for further details). Backup solutions are the shaped pupil masks (Vanderbei (2003)) which are of the most simplest implementation. The huge drawback of this solution is the poor inner working angle and possibly the associated outer working angle which may be a serious problem regarding its behavior against phase aberrations. Other solutions such as the focal plane band limited masks (Kuchner & Traub, 2002) may also be worth considering for the SPICA coronagraph (although the pupil shape may severely reduce the throughput).

5. Performance estimation

Some preliminary simulations were performed including the actual telescope specifications: telescope pupil shape, primary mirror surface roughness/bumpiness, tip-tilt jitter. The mirror surface accuracy is currently set to 0.35μm RMS, which is roughly the Rayleigh criterion for diffraction limited images at the lowest wavelength (5μm). Under these conditions, an additional deformable mirror (DM) is mandatory to correct for these imperfections with the additional difficulty of an operation temperature of 4.5K. ISAS is planing some cryogenic tests with MEMS DM from Boston Micromachines Corporation (36 element DM matrix). The electrostatic actuation is more suitable for cryogenic environment, contrarily to piezo actuators which stroke severely decreases at these temperatures. The simulation shown on Figure 1 is a preliminary result obtained with a 3 stages PALC and a 1.6 λ/D mask radius. The wavefront has a RMS bumpiness of 0.35μm which spatial power spectrum has an inverse power law ($f^{-2.5}$). It is corrected by a DM with 400 actuators (20 across the pupil) and a RMS accuracy of 8nm. The number of actuators of the DM allows spatial frequencies to be corrected up to $10\lambda/D$. This determines the OWA as long as the residual phase errors beyond these spatial frequencies are higher than the corrected part of the spectrum which is currently the case (the corrected part of the phase spectrum is flat except for the residual phase bumpiness). The high specified bumpiness of the primary mirror (0.35μm) actually limits the coronagraphic performance in an absolute way. Reducing the mirror polishing specification is also one of the current discussion point for the coronagraphic mission.

https://doi.org/10.1017/S1743921306009550 Published online by Cambridge University Press

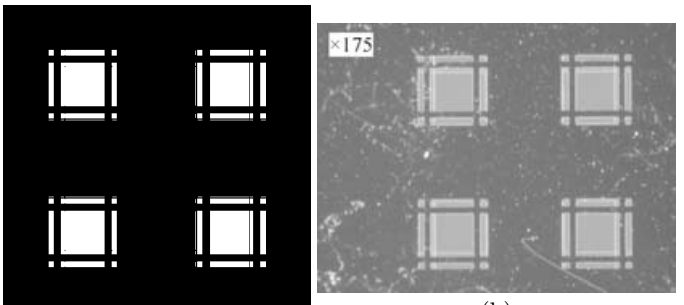

(a) (b)

Figure 2. Theoretical (a) and manufactured (b) binary pupil mask. The defects of (b) appear larger that what they actually are due to the slight defocus and light saturation at these location.

6. Laboratory experiments

6.1. *Binary shaped pupils masks*

Binary shaped pupil (Jacquinot & Roizen-Dossier, 1964) masks were invented and largely experimented in the 60's as ways to strongly attenuate the diffraction halo in optical systems by diffracting the light along preferential directions. More recently, binary shaped pupils of various kinds appeared, some of them recalling binary versions of linear apodizers which are commonly used in laser experiments in order to convert gaussian beams into flat beams for example (so called *beam shaping* techniques). Binary shaped pupil masks offer the advantage of being achromatic, meaning that the effect is in principle similar regardless of the wavelength. The other advantage of pupil masks is that they are very poorly sensitive (marginally sensitive) to tip-tilt errors/pointing errors. Indeed, in this case, and contrarily to other "focal plane" coronagraphs for example, the coronagraphic image is here invariant by translation, meaning that the convolution product between the object intensity distribution and the coronagraphic impulse response is preserved. The binary masks are usually designed as the solution of a system of non linear equations under a minimization/maximization criteria: maximize the throughput of the system, and minimize the intensity level in a given spatial area in the image plane. Some mathematical tools have been developed to numerically solve this kind of problems. For example, Vanderbei (2003) uses the AMPL mathematical programming language in association with the LOQO solver (Vanderbei, 1999). A variety of "unusual" pupil shapes can be obtained through this process as shown for example in Kasdin *et al.* (2003).

One of these masks have been fabricated by the *National Institute of Advanced Industrial Science and Technology* using ion etching process. The chosen test design was chosen to be of the type "checkerboard" or "bar-code" (Vanderbei *et al.*, 2004). This mask has a very large inner working angle (8 λ/D) because it was designed to match the current 30% central obscuration of the SPICA telescope. Future mask designs will consider 20% central obscuration telescope which enables a smaller IWA. The prototype mask (first attempt) is shown on Figure 2. Although many small defects are present, the PSF exhibits peak-to-valley contrast ratio of 10^{-5} along the diagonal direction relative to the mask orientation (horizontal direction of Figure 4). Note that these results were obtained after some optical setup tunings, and after the IAU meeting was held, thus improved by a factor of 10 from the previous results, as shown in Enya *et al.* (these proceedings). Improvements of the optical setup as well as the wavefront compensation by a DM is envisaged as future upgrades. A more detailed study of optimal checkerboard mask design for the SPICA coronagraph is described in Tanaka et al. (these proceedings).

https://doi.org/10.1017/S1743921306009550 Published online by Cambridge University Press

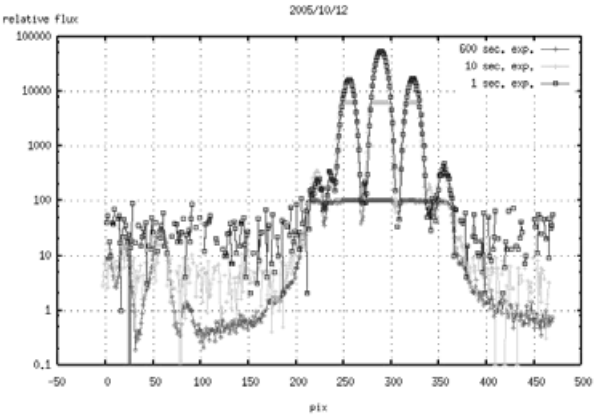

Figure 3. AIST mask PSF profiles along the diagonal of the mask orientation.

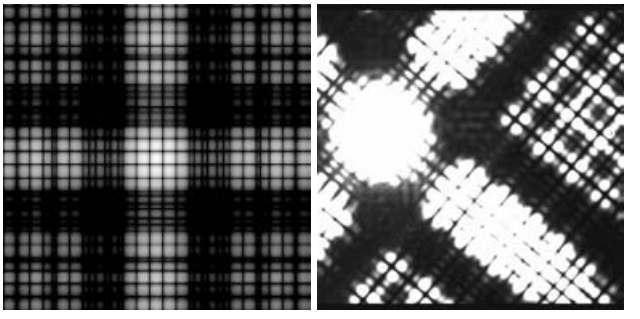

(a) (b)

Figure 4. (a) Theoretical PSF for the mask of Figure 2-a (logarithmic gray level stretch). (b) Actual laboratory recording of the binary pupil mask PSF obtained with the AIST mask (Figure 2-b) displayed as a linear gray level scale. The corresponding pupil mask is shown on Fig. 2. The theoretical PSF achieves a 10^{-7} contrast ratio in the 4 "corner areas" whilst $\sim 10^{-5}$ was obtained in the experiment.

6.2. *Multi-stage Pupil Apodized Lyot Coronagraph*

The prolate apodized Lyot coronagraph has been proposed by Aime *et al.* (2002). This elegant method is based on the mathematical properties of prolate spheroidal functions (Slepian & Pollak, 1961) which are invariant by Fourier transform, even if the original function is truncated (i.e. has a finite definition domain as it is the case for a given optical system pupil). The formalism of prolate apodized Lyot coronagraphy is extensively described in Aime *et al.* (2002), Soummer *et al.* (2003) and won't be detailed here. These authors also evidenced that the residual amplitude distribution in the Lyot plane (coronagraphic pupil) for a matching (unique) combination of apodizer prolate function and Lyot focal plane occulting mask diameter, is also a prolate function, and is still valid when a central obstruction is present (Soummer, 2005). Moreover this amplitude residual is the same prolate function as the entrance pupil one, but with a reduced amplitude, corresponding to the efficiency of the coronagraph. This very nice property directly leads to the multi-stage setup, where only one entrance pupil apodizer is used, but with a cascading number of identical Lyot occutling masks/Lyot stops combinations. Each stage provides the same rejection efficiency $\mathbf{Q}$, leading to a final rejection $\mathbf{Q}^{\mathrm{N}}$ if N stages are used. Consequently, if several stages can be used, then some very small occulting masks can be used, as small as 2 λ/D in diameter, as we plan to test in laboratory.

https://doi.org/10.1017/S1743921306009550 Published online by Cambridge University Press

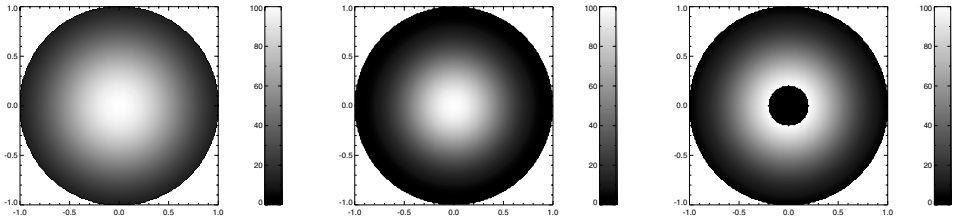

(a) (b) (c)

Figure 5. Three configurations of MS-PALC apodizers that are planned for laboratory tests. (a), (b) and (c) are respectively associated to $2\lambda/D$, $3\lambda/D$ and $3\lambda/D$ occulting mask diameters.

Finally, the MS-PALC offers several advantages but at the expense of some drawbacks so that a tradeoff must be found. The NAOJ and ISAS are setting up an experiment to validate this concept in laboratory. Several masks have been designed to test several configurations. The focal mask sizes vary from 2 to 3 λ/D in diameter, providing effective inner working angles of 1 to 1.5 λ/D respectively. Furthermore, the Lyot stops do not need to be undersized (in theory) so the overall throughput is defined by the entrance pupil apodizer only. Our apodizers throughput range from 20 to 35%.

The masks are currently being manufactured by Canyon Materials Inc. with the HEBS-glass technology. The HEBS substrate contains a superficial layer which can be opacified when bombarded with an electron beam. Details about this fabrication process can be found on the company website (Canyon Materials Inc.). Some encouraging coronagraphic results were already obtained with HEBS-glass focal plane masks (see Balasubramanian *et al.* in these proceedings). Although we might experience some problems with the phase delay introduced by the HEBS-glass pupil apodizer (Halverson *et al.*, 2005), this should be fixed by the future use of a DM (e.g. the already mentioned BMC mirror, or with a higher number of actuators).

References

Aime, C., Soummer, R., & Ferrari, A. 2004, *A&A* 389, 334
Aime, C. & Soummer, R. 2004, *SPIE Proc.* 5490, 456
Canyon Materials Inc., http://www.canyonmaterials.com/
Gay, J. & Rabbia, Y. 1996, *Comptes Rendus de l'académie des Sciences* t332, SérieII, 265
Guyon, O. 2004, *A&A* 404, 379
Halverson, P., Ftaclas, M., Balasubramanian, K., Hoppe, D., & Wilson, D. 2005, *SPIE Proc.* 5905
Jacquinot, P. & Roizen-Dossier, B. 1964, *Prog. Opt.*, 3, 29
Kasdin, J. 2003, *ApJ* 582, 1147
Kuchner, M. & Traub, W. 2002, *ApJ* 570, 900
Lyot, B. 1931, *Comptes Rendus de l'Académie des Sciences* 193, 1169
Nakagawa, T. 2000, *ISAS Report SP* 14, 189
Roddier, F. & Roddier, C. 1997, *PASP* 109, 815
Slepian, D. & Pollak, H. O. 1961, *Bell Sys. Tech. J.*, 40, 43
Soummer, R. 2005, *ApJL* 618, 161
Soummer, R., Aime, C., & Falloon, P.E. 2003, *A&A* 397, 1161
Tamura, M. 2000, *ISAS Report SP* 14, 3
Vanderbei, R. J. 2003, *ApJ* 590, 593
Vanderbei, R. J., Kasdin, J., & Spergel, D. 2004, *ApJ* 615, 555
Vanderbei, R. J. 1999, LOQO Users Manual, Version 3.10, *Optimization Methods and Software* 12, 485

https://doi.org/10.1017/S1743921306009550 Published online by Cambridge University Press